



Effect of Nanofillers on Conductivity and Electromagnetic Interference Shielding Effectiveness of High Density Polyethylene and Polypropylene Nanocomposites

Puttaraje Gowda Dinesh¹, Nijagal Marulaiah Renukappa², Tenzin Pasang³, Meghala Dinesh³ and Chikkakuntappa Rangananthaiah⁴

¹Department of Electronics and Communication Engineering, Dayananda Sagar College of Engineering, Bengaluru-560 078, Karnataka, India

²Department of Electronics and Communication Engineering, Sri Jayachamarajendra College of Engineering, Mysore -570 006, Karnataka, India

³Department of Studies in Physics, University of Mysore, Manasagangotri, Mysore-570 006, India

⁴Director of Research, Sahyadri Government Research Centre, Mangalore-575 007, India
dineshprg@gmail.com

ABSTRACT

High density polyethylene (HDPE) and polypropylene (PP) based nanocomposites were fabricated using a constant 20 wt. % of carbon black (CB) as the base and different wt.% (0.25 to 1) of multiwalled carbon nanotubes (MWNT). The conductivity and the electromagnetic interference shielding effectiveness (EMI SE) and nano size free volume cavities of conducting HDPE/PP nanocomposites and their interrelation is explored. We found that the resistivity decreases by ~13 orders of magnitude and EMI SE shows a maximum of -30 dB in the three nanocomposites as the loading of MWNT increases. We obtained higher value of EMI SE in PP based nanocomposite compared to HDPE based ones. X-ray diffraction (XRD) results indicated that HDPE is highly crystalline while PP is highly amorphous. Filler loading reveals changes in crystalline and amorphous contents in the nanocomposites. Differential scanning calorimetry (DSC) results support the findings of the XRD data. Free volume data derived from positron annihilation lifetime spectroscopy (PALS) exhibits a linear relation with EMI SE values of the three composite. Better EMI SE is achieved for PP composite without the use of functionalized MWNT with PAni.

Key words: Resistivity, electromagnetic interference shielding effectiveness, free volume, positron annihilation lifetime spectroscopy

INTRODUCTION

Electromagnetic interferences (EMI) is defined as the unwanted radiated electrical signals induced in electronic circuitry of electronic devices used in commercial, military, scientific communication instruments. The EMI brings in faulty actions or malfunction of the electronic equipments, medical apparatus, and industrial robots or even cause harm to human body and may become one of the public nuisances [1, 2]. Therefore, it is important to shield electrical and electronic devices from the EMI frequency spectrum to ensure proper functioning of the electronic devices. Traditionally, metals have been used as strong shielding materials because of high conductivity but suffer from disadvantages from the point of view of cost, weight, corrosion and molding properties. Further, metal shielding reflect radiation and is not suitable in applications where absorption is a prime requisite, e.g., in stealth technology, radar and microwave technology [3]. Owing to these drawbacks of metal EMI shielding, polymer composites containing conductive fillers have been developed in recent times as alternative EMI shielding materials since they come the advantages like light weight, low cost, resistant to corrosion and processing advantages.

However, in such materials, the EMI shielding effectiveness (SE) depends on many factors, including filler's intrinsic conductivity, filler loading, dielectric constant, aspect ratio and filler-polymer matrix interactions [4, 5].

We mainly deal with three mechanisms for EMI shielding: namely attenuation, reflection (multiple reflections), and absorption [5]. The primary mechanism is reflection; reflection requires the existence of mobile charge carriers (electrons or holes) which interact with the electromagnetic radiation. Thus the shield tends to be electrically conducting, though a high conductivity is not required for shielding. Conduction requires connectivity in the conduction path, whereas shielding does not [6]. The reflection loss is a function of the ratio σ_r/μ_r where σ_r is the electrical conductivity relative to copper and μ_r is the relative magnetic permeability. The second mechanism of EMI shielding, namely absorption, requires electric and/or magnetic dipoles which interact with the electromagnetic fields. The electric dipoles may be provided by materials having high dielectric constants or magnetic permeability [5]. The absorption loss is a function of the product $\sigma_r\mu_r$. Unlike reflection where the loss decreases with increasing frequency, the absorption is the opposite that is loss increases with increasing frequency. The absorption loss is proportional to the thickness of the shield. The other mechanism is attenuation and multiple reflections. This refers to the reflections at various surfaces or interfaces in the shield. This mechanism requires the presence of a large surface area or interface area as in a porous or foam material, or a composite material containing filler which has a large surface area for the shield.

In recent times researchers have tried three types of carbonaceous fillers, i.e., carbon black (CB), carbon fiber (CF) and carbon nanotubes including multiwalled (CNTs/MWNTs) [7] with a suitable polymer matrix. In certain cases, pairs of fillers have been tried. The different structures and shapes of these conductive fillers and the morphologies of their dispersion will affect the ability to construct an effective conductive network, which is key to increasing the electrical conductivity of the polymer-filler composites [8-10]. Some researchers [11-13] have simultaneously introduced CB and CNTs into polymer matrices through conventional processing techniques.

Literature reveals that polymer composite with carbon nanotubes as filler provide -40 dB EMI SE at 10 GHz [14] while short carbon fiber filled composite also yielded -40 dB EMI SE at 10 GHz and reported to be more effective than multiwalled carbon nanotubes and carbon black filled composites [15]. Another work reports an exfoliated graphite in a polymer matrix produced -34 dB EMI SE at 27 GHz [16]. Zirconia-embedded carbon fiber resulted -32 dB at 5 GHz [17]. Interestingly, another work on composite with carbon fibers reported -30 dB EMI SE at a lower frequency of 1 GHz [18]. Another work reported -26 and -25dB at 1 GHz [19, 20]. However, the combined use of carbon black and short carbon fibers for the composite yielded only -26 dB at 1 GHz [21]. Graphene was also tried which resulted in about -20 dB at 10 GHz and -18 dB at 1-8 GHz range [22]. Use of coiled carbon nanotubes has been found to be more effective than the use of conventional carbon nanotubes, giving only -15 dB at 8 GHz [23]. Polystyrene based composite with carbon nanotubes in the form of foam was also tried for its lightweight character but found to be not suitable for EMI SE [24].

From the above survey of polymer based nanocomposites for EMI SE applications, we find that the results are varying dependent on several factors from the type of the polymer matrix to filler type and amount. However, much work has been done to introduce electrical conductivity in various polymer matrices but high percolation threshold and lower aspect ratios in comparison to metals remains a challenging issue. In this direction considerable work is still to be done to further improve EMI SE and mechanical properties of the conducting polymer based composites. The poor EMI shielding/microwave absorption properties are often correlated with aggregation effects and inter-particle contacts/interactions requires detailed studies. Efforts to understand the polymer-filler interaction are essential for the design of good shielding materials had to be addressed. However, the inherent nature of the polymer matrix namely the micro pores in its structure which plays an important role for good dispersion and conducting paths had been completely ignored. Therefore, knowledge of the micro pores or usually called free volume cavities and their role in dispersion, conductivity and EMI SE are very essential. Therefore, in the present work we made a comparative study of functionalized nanofiller in two polymer matrices HDPE and PP in the presence of 20 wt% CB in an effort understand how the conductivity, EMI SE and free volume cavities of conducting HDPE and PP nanocomposites are related. To study the connectivity of free volume to the aforementioned properties of the composites, we have employed positron annihilation spectroscopy to measure directly the free volume of the composites. XRD and DSC are employed to study the crystalline nature and the thermal behaviour of polymer nanocomposites respectively.

EXPERIMENTAL DETAILS

Materials

The polymers used in this work are high density polyethylene and polypropylene. The HDPE has melt flow index of 0.2 g/10 min, density =0.94 g/cc, melting temperature of 128°C, while the PP has melt flow index of 7-12 g/10 min,

density =0.90 g/cc, melting temperature of 180°C. The polymers were supplied by Honam Petrochemical Corporation, South Korea and GLS Polymers Pvt. Ltd., India respectively. The Carbon black particles were of size of 24 nm and Multiwalled carbon nanotubes were of 10-20 nm size with a length of 10-50 μm supplied from Korea Carbon Black Comp. Ltd., and Iljin Nanotech Comp. Ltd., South Korea, respectively. The nitric acid (60% purity), xylene and aniline monomer (99% purity) were sourced from Aldrich Chemicals, USA. The ammoniums per sulfate (APS), sodium dodecyl sulphate (SDS) were used without further purification in the processing.

Fabrication of Nanocomposites

The MWNT were first oxidized using nitric acid to yield the o-MWNT [25] and then HDPE-CB-MWNT nanocomposites were prepared by solution melt mixing process. The o-MWNT wt. % of 0.25, 0.5, 0.75 and 1.0 were mixed with the HDPE for precursor master batch by solution method using xylene as solvent prior to melt mixing. The prepared master batches were melt mixed with HDPE and 20 wt. % of CB using internal Haake mixer at 180°C with 60 rpm for 30 minutes of mixing time. Further, the blended mixture was hot pressed at 180°C into sheets with a thickness of ~0.35mm.

Similarly, the processing of HDPE-CB-PAni-MWNT nanocomposites was carried out as follows; the functionalization of the MWNT surface with a PAni was carried out according to the procedure outlined in literature [26]. The MWNT were oxidized using nitric acid to yield o-MWNT. Then in situ polymerization of aniline in the presence of o-MWNT gave a new MWNT coated PAni. The phenyl amine functional groups on the surface were grown into PAni chain, so that PAni functionalized the o-MWNT. The HDPE-CB-PAni-MWNT nanocomposites were prepared by solution melt mixing process. A wt% of 0.25, 0.5, 0.75 and 1.0 of PAni-MWNT were mixed with HDPE for precursor master batch by solution method using xylene as solvent, prior to the melt mixing. Prepared master batches were melt mixed with HDPE with 20 wt. % of carbon black using Haake mixer at 180°C with 60 rpm for 30 minutes. Further, the blended mixtures were hot pressed at 180°C into sheets having thickness of ~0.35mm.

The compounding of PP-CB-MWNT nanocomposites was carried out in a Brabender Plasticorder (model 83525) with a constant 20 wt. % CB filler and varying wt.% of MWNT in 0.25, 0.5, 0.75 and 1wt. % were made. The standard mixing time was 15 minutes and the speed during blending was 15 rpm at 175°C. After compounding, a batch of composites was pressed by compression molding at 220°C at a constant pressure. When the blends were completely melted, the ultimate pressure was maintained for 10 minutes and then cooled by water at the rate of about 20°C/ minutes until the temperature fell below 50°C.

For convenience, the samples are named as S-, H- and P-series respectively for HDPE-CB-MWNT, HDPE-CB-PAni-MWNT, and PP-CB-MWNT nanocomposites with varying amount of fillers. Details of this can be seen in Table 1.

MEASUREMENTS

X-ray Diffraction and DSC Measurements

The XRD is a powerful and nondestructive technique used primarily for crystallographic characterization of solid materials. It is based on Bragg's law [$2d\sin\theta = n\lambda$] and uses the position of the diffraction peak. XRD analysis was performed using Rigaku Corporation, diffractometer equipped with a point detector at scan increment of 0.01° and scan speed of 2 °/ minutes. A Cu K α beam (wavelength $\lambda = 1.54 \text{ \AA}$) was used as the radiation source. For this analysis, samples were taken in the form of a block having dimension of 10 mm \times 10 mm \times 0.35 mm.

The DSC is used to understand the thermal behavior of the samples. The DSC scans composite samples were measured using a DSC-Q200 apparatus of TA Instruments, USA, in nitrogen atmosphere. Samples of 6-10 mg weight were used in the DSC scan with a heating rate of 10°C/ minutes. DSC scans were taken in the temperature range 25°C to 220°C. The values of onset temperature (T_o), melting temperature (T_m), final temperature (T_f) and the area under the melt curve (for enthalpy, ΔH) of the composites have been arrived at.

Resistivity and EMI SE Measurements

The resistance of the samples so prepared was measured using CROPICO microhmmer with four probe method and Sefelec megohmmeter M1501M. The sample size of 50 mm diameters with 0.35 mm thickness was placed between electrodes for the measurement. The dc resistivity (ρ) is calculated using the formula,

$$\rho = \frac{RA}{t} \Omega \cdot \text{cm} \quad (1)$$

where R is the resistance of the sample, A is the area of the electrode and t is the thickness of the sample. Then the dc conductivity (σ) is calculated as

$$\sigma = \frac{1}{\rho} \text{S/cm} \quad (2)$$

The EMI SE of the nanocomposites was measured through scattering parameter (S) measured in a two-port configuration. The sample of size 50 mm × 50 mm × 0.35 mm was placed between two coaxial wave guide adapters. Using the Agilent N 5230A PNA series (10MHz-50GHz) network analyzer, the S parameter, S_{11} and S_{21} were carried out over frequency range 6.5-10.5GHz. The output from the vector network analyzer was in terms of scattering parameters, S_{xy} . The first number in the suffix refers to the port at which the output is measured and the second number refers to where the signal originates from. S parameter values are used to calculate the transmitted and reflected power in percentage of input wave power in the two port configuration.

PALS Measurements

Positron Annihilation Lifetime Spectrometer (PALS) was used to measure the positron lifetime values in pure HDPE, PP and HDPE-CB-MWNT, HDPE-CB-PAni-MWNT and PP-CB-MWNT nanocomposites. The spectrometer consisted of a fast-fast coincidence system with BaF₂ scintillators coupled to photomultiplier tubes type XP 2020/Q with quartz windows as detectors. The BaF₂ scintillators were conically shaped to achieve a better time resolution. Two identical pieces of the samples (1cm x1cm x1mm) were placed on either side of a 17- μ Ci²²Na positron source which was deposited onto a pure Kapton foil 12.7 μ m thick. This sample-source sandwich was positioned between the two detectors of the spectrometer to acquire the lifetime spectrum. Typical spectrum accumulation time was 90 to 120 minutes. The operation details, data acquisition procedure and free-volume parameter calculations etc. can be found in References [27, 28].

RESULTS AND DISCUSSION

XRD Results

The XRD spectra clearly show that HDPE based nanocomposites are crystalline in nature and the PP nanocomposites are of semi crystalline nature as evident from Fig.1. HDPE has a low degree of branching and thus results in efficient packing of the chains into the crystal structure. The known crystal structures of polyethylene were found to be orthorhombic, monoclinic and hexagonal, depending on the processing conditions as reported in literature [29, 30]. The phase in which the polymer chains are nearly parallel and arranged in an order is known as the crystalline phase, which exhibits strong and sharp crystalline peaks in the XRD pattern. On the other hand, the phase where the chains are not aligned in an order and do not have close packing is known as the amorphous phase. The amorphous phase exhibits a shallow and broad peak in the XRD pattern [31].

The XRD spectrum of HDPE-CB nanocomposites shown in Fig. 1a-b has a strong peak at 21.53 ° ($d = 0.4124$ nm) and another less intense peak at 23.89 ° ($d = 0.372$ nm). CB filler is known to increase the crystallinity in HDPE [32] and present data is in agreement with this. With addition of MWNT, we observed a decrease in peak intensities indicating the decrease in the amount of crystalline phase of HDPE-CB in nanocomposites. The peak intensity of the HDPE-20 wt.% CB composite is 36564 cps, which comes down to 25323 cps with mere addition of 0.25 wt.% of o-MWNT to the composite. Further, with the addition of 1 wt.% MWNT the peak further reduces to 23340 cps at 21.54 ° ($d = 0.4121$ nm). Interestingly, we observed increased peak intensities when PAni-MWNT is added to the HDPE-CB. Since PAni is a conducting polymer it is bound to initiate more interaction between the filler particles and the polymer matrix. This results to some close packing resulting in increased crystallinity. This is evident from 0.25 wt. % PAni-MWNT added to HDPE-CB composite for which the main peak intensity goes to 37167 more than observed for HDPE-CB (36564). This further increase to 44489 cps with the addition of 1 wt. % PAni-MWNT to the HDPE-CB matrix. These changes are well reflected in the free volume data discussed later.

Polypropylene is also orthorhombic unit cell structure but comes with helical as well as zigzag plain chain conformations. Due to this form of chain conformation certainly leads to less packing and hence amorphicity is more in PP. As we can see in PP nanocomposites, we observe an a broad peak at 20.14 ° (0.4412 nm) Fig.1c and second less intense broad peak at 23.24 ° (0.3823 nm) for PP loaded with 20 wt.% CB. There is slight increase in crystalline peak intensity with the incorporation of 0.25 wt. % MWNT Fig.1b but further addition of MWNT only resulted in decrease in the peak intensity. Thus, we can infer that with the increase in filler loading, the XRD intensity profile shows intensity increases in HDPE-CB-PAni-MWNT nanocomposites to a larger extent but less increase in HDPE-CB-MWNT and PP-CB-MWNT nanocomposites. Further we can state that functionalization of MWNT with PAni has a significant increase in crystallinity (as evidenced by peak intensity) of HDPE-CB-PAni-MWNT nanocomposites compared to others.

DSC results

The DSC curves for the HDPE-CB-MWNT nanocomposites with different contents of MWNT are shown in Fig. 2a-c. DSC curve and temperature range were same in the case of HDPE-CB-PAni-MWNT and PP-CB-MWNT which is not included here. T_m is the point at which the (now crystalline) polymer molecules have gained enough vibrational freedom to break free from the solid binding forces and form a liquid. Due to the increased freedom of these molecules, the DSC graph should take a sudden dip at this temperature to indicate the endothermic nature of the

process, which is a first order transition. Therefore the segmental motion will be more at this temperature. The values of onset temperature (T_o), melting temperature (T_m), final temperature (T_f) and change in enthalpy, (ΔH) obtained from DSC curves are tabulated in Table 1.

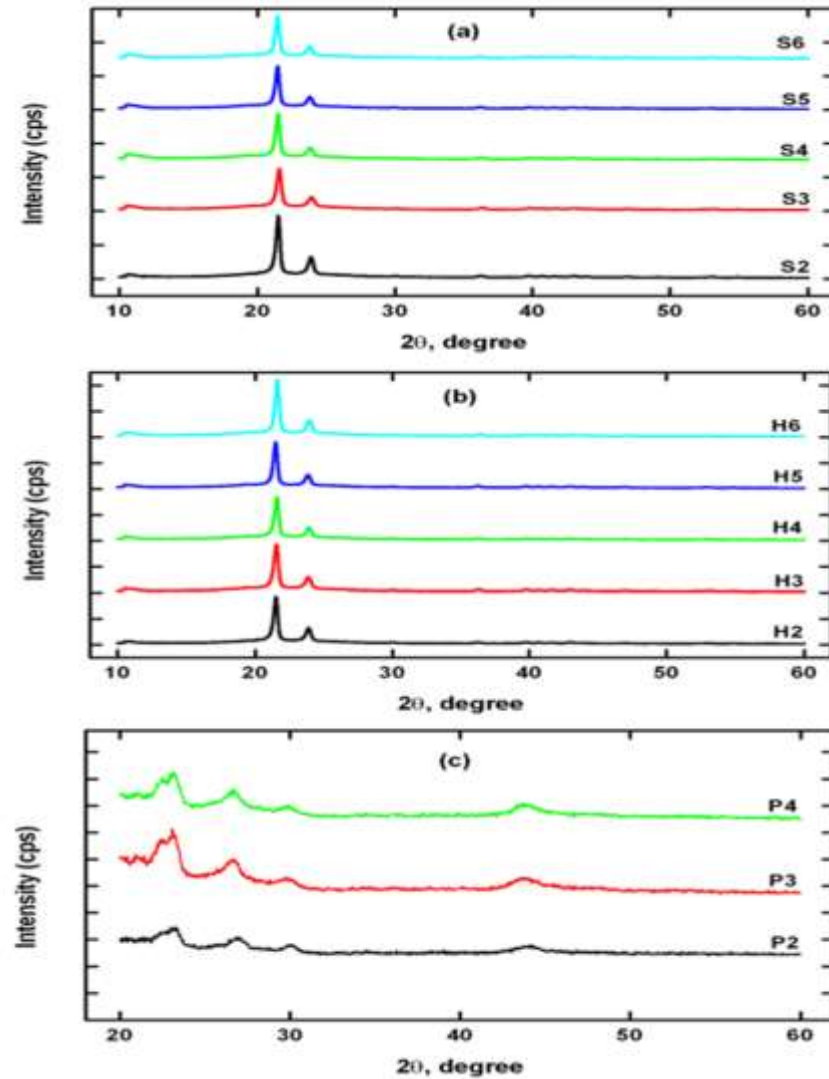


Fig. 1 X-ray diffraction patterns for HDPE and PP nanocomposites with varying amount of fillers

Table -1 Data from DSC of Nanocomposites

Sample composition and notation used		Transition temperature ($^{\circ}\text{C}$)			Enthalpy ΔH (J/g)
		T_o	T_m	T_f	
HDPE + 20 wt.% CB	S2 : Without MWNT	82	130	137	177
	S3 : 0.25 wt.% MWNT	82	127	135	143
	S4 : 0.5 wt.% MWNT	77	128	135	140
	S5 : 0.75 wt.% MWNT	76	128	135	136
	S6 : 1 wt.% MWNT	78	128	135	126
HDPE + 20 wt.% CB	H2 : Without PAni-MWNT	82	130	137	177
	H3 : 0.25 wt.% PAni-MWNT	117	130	138	148
	H4 : 0.5 wt.% PAni-MWNT	116	128	137	146
	H5 : 0.75 wt.% PAni-MWNT	116	130	136	143
	H6 : 1 wt.% PAni-MWNT	116	129	135	135
PP + 20 wt.% CB	P2 : Without MWNT	160	169	174	97
	P3 : 0.25 wt.% MWNT	164	172	176	78
	P4 : 0.5 wt.% MWNT	158	172	180	102
	P5 : 0.75 wt.% MWNT	159	170	176	76
	P6 : 1 wt.% MWNT	158	170	176	124

The HDPE normally exhibits the onset temperature T_0 at 115 °C and melting temperature T_m at 134 °C [33]. From Table 1, it is clear that there is a small decrease of T_m with incorporation of 20 wt. % CB and further small decrease with MWNT in the polymer matrix. However this seems to suggest that the change is small and hence the original crystal structure of the host matrix may not be altered very much in the presence of CB and MWNT. However we observe considerable decrease in the enthalpy (ΔH) from 293 J/g for pure HDPE [34] to 177 J/g when HDPE is added with 20 wt. % of CB. This further decreases 126 J/g for 1wt. % MWNT. However with 1wt. % PANi-MWNT in the polymer matrix enthalpy is 135 J/g. We observe positive enthalpy; the melting process is endothermic which the case is generally. However no T_g has been observed either for HDPE or PP nanocomposites. Thus, the decrease of both XRD peak intensity and the enthalpy of fusion are probably due to the decrease in the crystalline nature of HDPE matrix [35]. Upon heating in xylene, the HDPE molecular chains are relaxed and the nanocomposite formed has relaxed HDPE chains. Further this observation can be attributed that in the nanocomposites there is a disturbed continuity of the HDPE chains. Similar studies are also reported in the HDPE/carbon nanotube composites by other researchers [36, 37].

For PP based nanocomposites, polypropylene has a melting temperature of 160°C [33] and as can be seen from Table 1, unlike in HDPE nanocomposites there is an increase in the melting temperature starting from just 20 wt. % CB in the PP matrix. Additionally we observe a significant increase in ΔH from 75.34 J/g in pure PP to 97 J/g in the 20 wt. % CB incorporation. ΔH values further increases up to 124 J/g upon loading of 0.25-1 wt. % MWNT. We observed that the crystalline nature of composites increase with addition of CB and MWNT to PP matrix slightly. The results in the Table 1 indicate that the additions of MWNT to PP+20 wt. % CB matrix results indicate that both T_0 and T_m increase by about 4 °C. Interestingly, we observe from the graph that a small shift in T_m towards higher temperature which is relatively more for the composites with lower MWNT content (e.g. 0.25 wt.%) as compared to those with higher MWNT. Thus, the nucleation effect of MWNT in PP is not very significant for MWNT content \geq 0.5 wt. %. Seo and co-workers had also reported that the addition of \geq 1 wt. % multiwalled carbon nanotubes enhances the nucleation process during PP crystallization [38, 39].

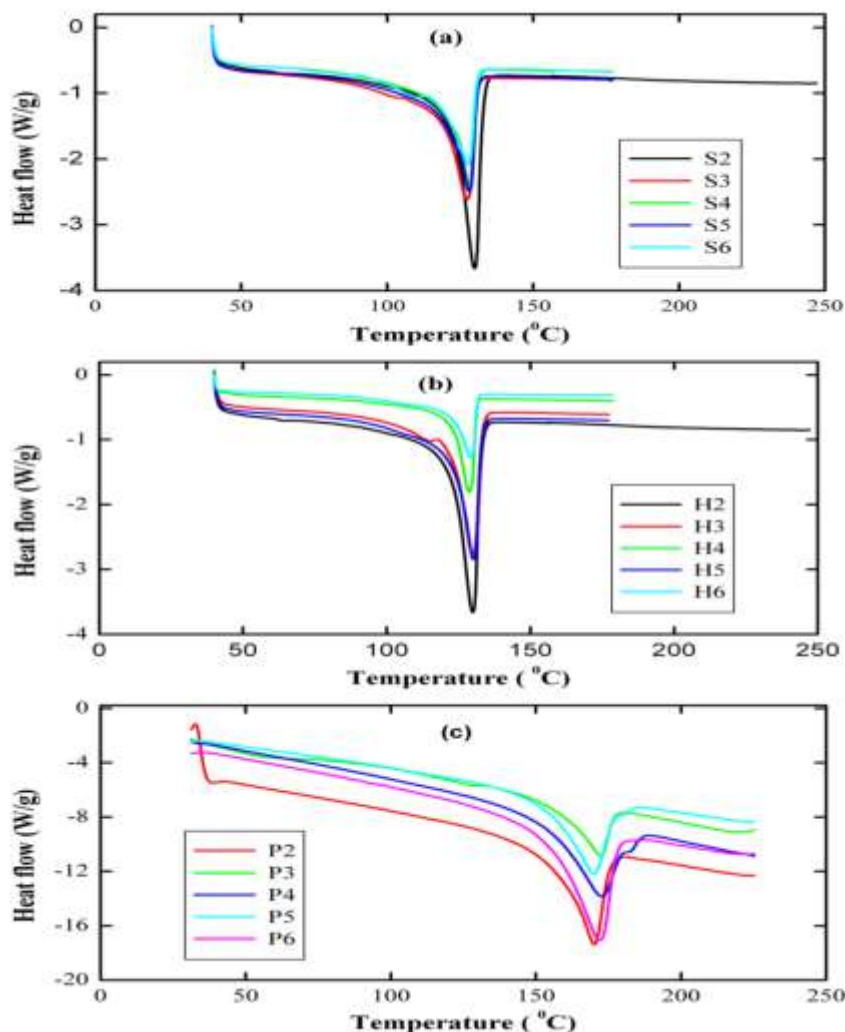


Fig. 2 DSC curve for HDPE and PP nanocomposites with varying amount of filler

Resistivity

In Fig. 3 we show how the resistivity varies as a function of MWNT filler loading in HDPE and PP nanocomposites with a constant 20 wt. % CB. As can be seen from the Fig.3, the resistivity of three types of nanocomposites namely HDPE-CB-MWNT, HDPE-CB-PAni-MWNT and PP-CB-MWNT exhibits a decreasing tendency in comparison to base material namely polymer matrix with constant 20 wt. % CB. On the other hand, addition of MWNT, we observe a marginal decrease in resistivity. The drastic change in resistivity with the addition of 20 wt. % of CB to HDPE and PP matrix suggest the possibility of discrete conductive aggregates which seems finally grow into a continuous conductive chain at the critical concentration known as percolation threshold. When conductive filler concentration increases above percolation threshold, there will be an increase in the number of such chains. The large number of continuous conductive chains leads to the formation of mesh of conductive networks. Therefore, when the first conductive chain is formed at the percolation (beyond 0.25 wt. % of MWNT) the system behavior could change from insulating to conductive and an abrupt decrease in the resistivity is observed. This is clear in composites with 0.5 wt. % MWNT onwards. However, at loading beyond percolation, it appears that the number of conductive chain might increase, but the increase in conductivity is marginal.

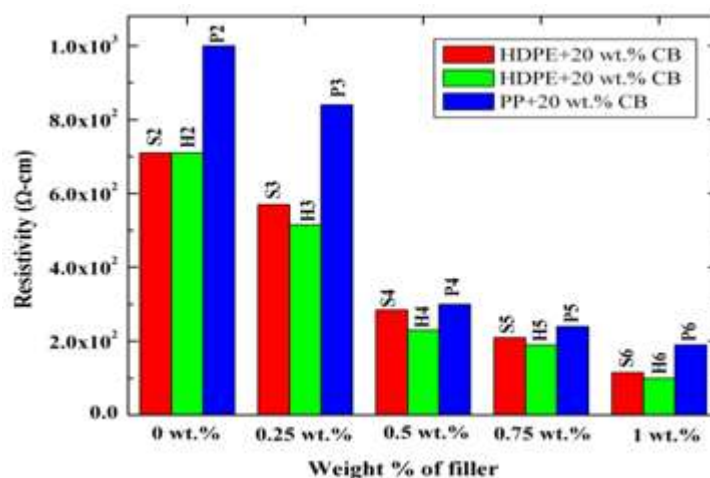


Fig. 3 Resistivity of HDPE-CB-MWNT, HDPE-CB-PAni-MWNT and PP-CB-MWNT nanocomposites as a function of MWNT and PAni coated MWNT as filler loading

Electromagnetic Interference Shielding Effectiveness (EMI SE)

The term 'shielding' is used to describe the effective blocking of EMI. This is provided by a conductive medium that reflects, absorbs, or transmits the electromagnetic interference to the ground. The shielding effectiveness expressed in dB value is an important parameter of electromagnetic shielding material. It is dependent upon many parameters as described earlier in the introduction. The SE of composites depends both on the type and amount of filler as well as the nature of polymer matrix. The filler concentration plays the major role but other factors like the particle size, shape and structure, aspect ratio, filler orientation, filler-matrix interaction and processing techniques do influence SE [40]. The EMI SE of different composites containing 20 wt. % of CB and varying amounts of MWNT (0.25 to 1 wt. %) as fillers over the frequency range of 6.5-10.5 GHz has been investigated in this paper and discussed below.

Effect of Frequency on EMI Shielding Effectiveness

The EMI SE of the HDPE and PP nanocomposites with a constant 20 wt. % of CB in the matrix in the frequency range 6.5-10.5 GHz is shown in Fig. 4. It is observed that the EMI SE of all the nanocomposites shows an oscillating behavior against frequency with the highest EMI SE around negative 25-30 dB. The oscillatory nature seems to decrease in the high frequency domain. We do find such reports in literature [41-43] particularly at lower frequencies (<10 GHz). The variation of EMI SE against frequency below 10 GHz is non linear in character suggesting that the shielding effectiveness of the nanocomposites is not stable with frequency of incident wave. This is possibly due to irregular nature of conductive networks established in the composite structure an opinion expressed by several in works [41, 43]. Another reason could be due to the fact that when composite is placed in an electromagnetic field, three competing processes namely reflection (multiple reflections) absorption and transmittance will be in operation. Since the EMI SE is the net result of these processes, it is not easy to expect a definitive relationship to operate as these three processes are not linear with frequency.

As described earlier, we know that the EMI SE is proportional to conductivity and permittivity of the material [44]. Both these properties depend on composition of the composite and hence affect the EMI SE values. The distribution

of the filler in the polymer matrix determines the void space between the fillers or their aggregates which in turn depends on the free volume of the polymer matrix. If high shielding is to be achieved, the conductive particles or fibers should form a close packed array throughout the matrix more like a conducting mesh [44-46]. Although, SEM pictures could reveal the dispersion, it pertains to only the surface morphology of the nanocomposites but not the bulk matrix. That is why we did not go for SEM studies of our composites instead we exploited the free volume properties which is a bulk property. The results from PALS are presented in the next section. If close packing due to presence of fillers happens, we shall see the fractional free volume should decrease and that is observed for the composites at few compositions. The voids in the conductive composite affect absorption and return loss due to their effect on internal reflection. The dependency of EMI SE of the composites will be discussed in the light of positron results in the next section.

In the present study, we found that for all the three types nanocomposites a marginal increase in EMI SE value with increasing content of MWNT in the composite. In this the contribution to the EMI shielding from the 20% of CB in the composites cannot be ignored. The highest SE measured is -27.26 dB at 6.8 GHz for HDPE-CB-MWNT nanocomposite. Surprisingly we did not find higher values for PANi treated MWNT composite since we observed -27.63 dB at 6.8 GHz for HDPE-CB-PANi-MWNT with 1 wt. % MWNT in the sample. However for PP-CB-MWNT nanocomposites (1 wt. % MWNT), the highest SE measured is -29.27 dB at 6.8 GHz. Therefore, we found that the EMI SE is higher in PP composites compared to HDPE composites probably the filler is distributed in the highly amorphous PP compared to HDPE. Because of this, a decrease in the average distance between fillers in the amorphous phase where the chains are more flexible and disordered leading to a more efficient conductive network. However, the network may not be uniform throughout the matrix and as such the SE exhibits oscillatory behaviour as a function of frequency. If the number of meshes increases and mesh size decreases, the EMI SE is expected to be progressively increasing [47]. However, in the present study this issue has not been looked into. Another aspect we see from Fig. 4 is that as the frequency increases, the EMI SE decreases but the magnitude of oscillating behaviour also decreases. Since the wavelength of the microwaves becomes shorter at higher frequencies, the electromagnetic wave can penetrate the conducting mesh easily and as such the EMI SE decreases at higher frequencies [48]. Therefore, it becomes clear that frequency dependency of EMI SE is due to the distribution of the conducting filler in the polymer matrix.

Relationship between Free Volume, Conductivity and EMI SE

Polymer nanocomposites are multiphase systems in which trapping of positrons/positronium at sites like polymer-nanoparticles interfaces and the native nano size free volume cavities in the base HDPE and PP matrices occur. Positron lifetime spectroscopy is an established tool to investigate defects in metals, oxides and free volume in polymers and polymer based materials [49]. For the meaningful interpretation of conductivity and EMI SE in the nanocomposites, we have measured positron annihilation lifetime parameters in the HDPE, PP with a constant 20 wt. % CB and varying filler loading.

The PALS spectra were analyzed using the computer program PATFIT-88 [50]. This software decomposes a PALS spectrum into three discrete lifetime components τ_1 , τ_2 , and τ_3 with respective intensities (probabilities) I_1 , I_2 and I_3 . The general attribution of these lifetime components is well established and is as follows: the shortest lifetime τ_1 with intensity I_1 corresponds to para-Positronium (*p*-Ps) and free positron annihilations. The lifetime component τ_2 with intensity I_2 is due to trapping of positrons at the crystalline defects. The longest lived component τ_3 with intensity I_3 is due to pick-off annihilation of the ortho-Positronium (*o*-Ps) from the free volume cavities present mainly in the amorphous regions of the polymer matrix. Nakanishi [51] suggested relation (Equation (3)) which is based on the earlier works of Tao [52] and Eldrup [53.] to connect τ_3 with the radius of the free volume cavity. We have used this relation to calculate the free volume cavity radius (R) from the measured τ_3 values.

$$\frac{1}{\lambda_3} = \tau_3 = 0.5 \left[1 - \frac{R}{R + \Delta R} + \frac{1}{2\pi} \sin \left(\frac{2\pi R}{R + \Delta R} \right) \right]^{-1} \text{ ns} \quad (3)$$

Here ΔR is the fitting parameter and has been evaluated to be 1.656 Å from the available molecular media [28]. The free volume cavity size is evaluated as $V_f = (4/3) \pi R^3$. The fractional free volume or the free volume content in percent (F_v) of the polymer system is then calculated as $F_v = CV_f I_3$, where C is a constant whose value is taken as 0.0018 Å⁻³ [28, 54].

The conductivity, EMI SE, *o*-Positron life time (τ_3) free volume size (V_f) and fractional free volume data for the nanocomposites are presented in Table 2.

Table -2 Conductivity, EMI SE and Positron Annihilation Lifetime Parameters of Nanocomposites

Composition (wt.%)		Conductivity (S/cm)	EMI SE (dB) at 6.8GHz	τ_3 ± 0.02 (ns)	I_3 ± 0.2 (%)	V_f ± 0.01 (\AA^3)	F_v ± 0.04 (%)
HDPE	Pure HDPE	-	-	2.15	17.34	111.96	3.49
	S2	1.38×10^{-3}	24.32	2.03	4.39	100.37	0.79
	S4	3.79×10^{-3}	24.95	2.16	7.09	112.87	1.44
	H4	4.35×10^{-3}	26.29	2.10	4.75	107.09	0.92
	S6	7.04×10^{-3}	27.26	2.18	7.47	114.91	1.54
	H6	5.71×10^{-3}	27.62	2.08	6.26	105.14	1.18
PP	Pure PP	-	-	2.20	14.33	116.86	3.01
	P2	9.09×10^{-4}	25.13	2.14	10.12	110.96	2.02
	P4	3.36×10^{-3}	28.72	2.18	10.72	114.91	2.22
	P6	4.76×10^{-3}	29.57	2.08	8.76	105.14	1.66

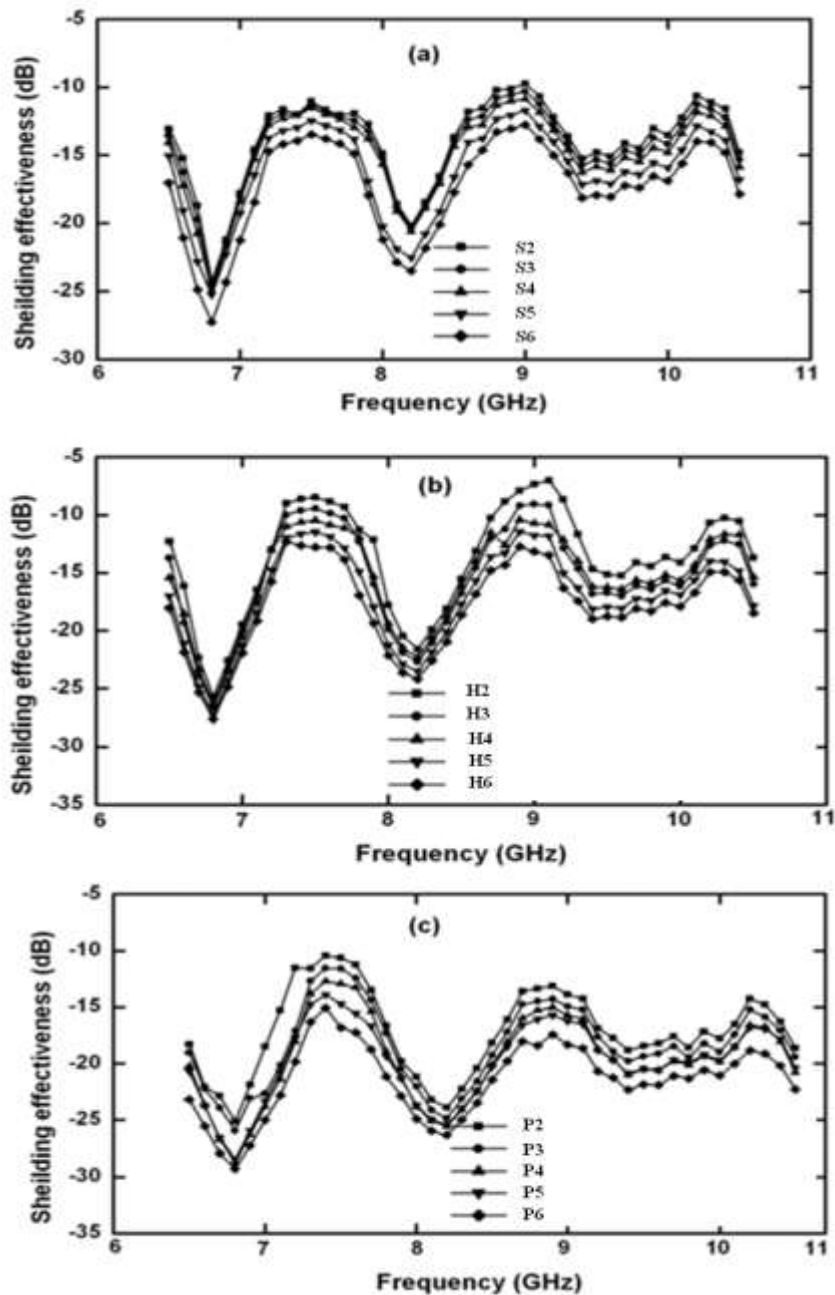


Fig. 4 EMI SE of a) HDPE -CB-MWNT b) HDPE-CB-PAni-MWNT and c) PP-CB-MWNT nanocomposites

The conductive materials like metals exhibit high EMI SE mainly due to reflection of the electromagnetic radiation. Lossy dielectrics like conductive composites exhibit low EMI SE because of absorption. It has been also found that EMI SE increases with conductivity of these composites [55]. However, the relation between EMI SE and conductivity is not linear rather it is exponential in nature [41]. This relation between EMI SE and conductivity raises the question; which factor the EMI SE is exclusively dependent on?; Is it really conductivity or some other factors play important roles in controlling EMI SE of conductive nanocomposites. From the data in the Table 2, we tried to check this connectivity. It can be seen that both conductivity and SE increased with increasing MWNT loading, but conductivity did not change significantly beyond the percolation threshold (~0.25 wt. %) while SE kept on increasing with increasing filler loading. This suggests that the number of percolating networks increased with increasing MWNT loading which interact with incident radiation leading to increasing SE without affecting the conductivity of the material. If we carefully observe the data in Table 2, we find that at the same level of conductivity, the EMI SE is higher in PP nanocomposites compared to HDPE nanocomposites. This could be possibly due to the fact that the filler may be pushed from crystalline phase of PP to the rich amorphous phase which decreases the average distance between CB-MWNT and hence PP favours the formation of a more efficient conductive network in nanocomposites which not so the case in HDPE case because it is highly crystalline as evidenced from XRD data.

The changes in *o*-Ps lifetime data can be seen reflecting the presence of nanofiller in polymer matrix resulting in increased or reduced free volume. From Table 2, we see that for pure HDPE, the fractional free volume is 3.49% which reduces to 0.79% upon 20 wt. % CB added to the matrix. Although the CB particles are of 24 nm size which cannot occupy the smaller native free volume cavities, but located between the chains such that the overall fractional free volume decreases by nearly 22%. Further adding the MWNT to this matrix increases the F_V because the length of the MWNT is 10-15 μm . F_V further increases on a smaller scale with increase in filler loading. However, depending upon the chain rearrangement upon filler loading, some close packing may result which indicates decreased free volume or vice versa if close packing results. This is more or less the same pattern for the other two types of nanocomposites as evident from the Table 2. The decrease of F_V is also indicative of the interaction between the filler and the polymer matrix in the form of cross links. If cross links occur, the polymer chains are brought closer which results in decrease of the free volume [27, 54].

To check any correlation between the fractional free volume and the EMI SE, which is reported for the first time, we made a selection of the SE and the corresponding F_V for each of the three nanocomposites in which F_V is the smallest. The reason is as stated earlier, filler –matrix interaction results in reduced F_V . These are and shown in Fig. 5. As can be seen, the data fits into a linear relation of the type $F_V = 0.23(\text{EMI SE}) - 5.067$ with $R^2=0.996$. So, the EMI SE falls as the fractional free volume falls. On the other hand, if the fractional free volume is more, the conductivity in the sample increases due to many more pathways created for conducting charges. Interestingly, this also means conductivity is more in such samples. Therefore, it can be inferred that the fractional free volume holds the key to the design of shielding materials having higher fractional free volume with the incorporation of nanofiller. The results indicate that due to high surface area of the filler particles (10-20 nm size) but of length 10-50 μm not many favorable interactions between filler and HDPE/PP matrices have been established. If the interactions increase, reduced F_V is expected and hence the EMI SE also gets reduced. Therefore, a balanced compromise is required for designing new polymer based nanocomposites for shielding purposes.

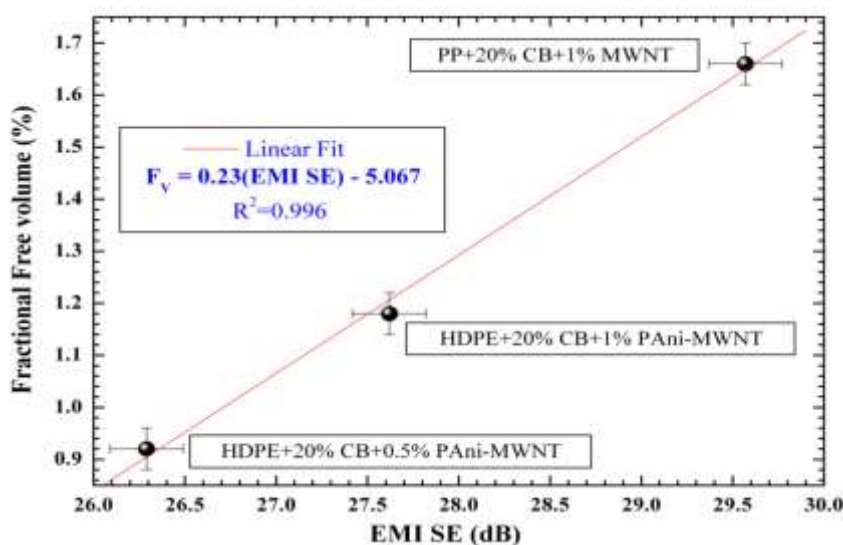


Fig. 5 Plot of fractional free volume versus EMI SE

CONCLUSION

Following conclusions are drawn based on the present experimental results:

- Formation of conductive network from the conductive particles in polymer matrix seems to be the key factor for increasing conductivity in polymer nanocomposites which leads to higher EMI SE. Closer the conductive mesh formed better will be the EMI SE.
- The EMI SE of all the nanocomposites showed dependence on filler loading and frequency domain. The oscillatory nature of EMI SE as a function of frequency suggests the random nature of conductive networks formed in the composite. The total shielding efficiency of ~30 dB indicates that these materials could be utilized effectively over a frequency range of 6.5-10.5 GHz.
- XRD results shows that addition of filler increases the crystallinity of HDPE-CB-PAni-MWNT nanocomposites whereas crystallinity decreases in the case of only MWNT loaded HDPE and PP nanocomposites.
- DSC results showed non existence of any glass transition but the melting curves exhibited large changes in enthalpy of melting suggesting that upon loading there is a rearrangement of chain conformations to accommodate the fillers. The decrease of both XRD peak intensity and the enthalpy of fusion are probably due to the decrease in the crystalline nature of HDPE based nanocomposites. There is an opposite trend in enthalpy indicating that MWNT act as nucleation sites for the crystallization of PP based nanocomposites.
- The positron results in terms of fractional free volume hold the key for the design of shielding materials having larger fractional free volume after filler incorporation resulting in higher EMI SE. However, more such studies are essential to arrive at a compromise between Fv and EMI SE for a given polymer matrix by suitable selecting the size and shape of the fillers.

Acknowledgements

The authors are grateful for the financial assistance granted by Visvesvaraya Technological University (VTU), Belgaum, under Research Grants Scheme for the Research project, Ref. No. VTU/Aca/2010/A-9/11325 dated 07-12-2010. One of the authors (TP) acknowledges the financial support from The Tibetan Children's village society. Further the authors are thankful to JSS Research Foundation, Mysore for the support and encouragement. The financial support provided to CR as Visiting Professor under CPEPA project of UGC is thankfully acknowledged.

REFERENCES

- [1] N C Das, T K Chaki, D Khastgir and A Chakraborty, Electromagnetic Interference Shielding Effectiveness of Ethylene Vinyl Acetate Based Conductive Composites Containing Carbon Fillers, *Journal of Applied Polymer Science*, **2001**, 80, 1601-1608.
- [2] Y Wang and X Jing, Intrinsically Conducting Polymers for Electromagnetic Interference Shielding, *Polymer Advanced Technology*, **2005**, 16, 344-351.
- [3] P Saini, V Choudhary, B P Singh, R B Mathur, and S K Dhawan, Polyaniline-MWCNT Nanocomposites for Microwave Absorption and EMI Shielding, *Material Chemistry and Physics*, **2009**, 113, 919-926.
- [4] J Joo and C Y Lee, High Frequency Electromagnetic Interference Shielding Response of Mixtures and Multilayer Films Based on Conducting Polymers, *Journal of Applied Physics*, **2000**, 88,513-518.
- [5] D D L Chung, Electromagnetic Interference Shielding Effectiveness of Carbon Material, *Carbon*, **2001**, 39, 279-285.
- [6] J Wu and D D L Chung, Improving Colloidal Graphite for Electromagnetic Interference Shielding Using 0.1 mm Diameter Carbon Filaments, *Carbon*, **2003**,41,1309-1328.
- [7] W Thongruang, R J Spontak and C M Balik, Correlated Electrical Conductivity and Mechanical Property Analysis of High-Density Polyethylene Filled with Graphite and Carbon Fiber, *Polymer*, **2002**, 43, 2279-2286.
- [8] R X Wang, X M Tao, Y Wang, G F Wang and S M Shang, Microstructures and Electrical Conductance of Silver Nano Crystalline Thin Films on Flexible Polymer Substrates, *Surface and Coating Technology*, **2003**, 204, 1206-1210.
- [9] S M Shang, W Zeng and X M Tao, Highly Stretchable Conductive Polymer Compositing With Carbon Nanotubes and Nanospheres, *Advanced Material Research*, **2010**, 123,109-112.
- [10] Z Spitalsky, D Tasis, K Papagelis, and C Galiotis, Carbon Nanotube-Polymer Composites: Chemistry, Processing, Mechanical and Electrical Properties, *Progress in Polymer Science*, **2010**, 35, 357-401.
- [11] Y Sun, H D Bao, Z X Guo, and J Yu, Modeling of the Electrical Percolation of Mixed Carbon Fillers in Polymer-Based Composites. *Macromolecules*, **2009**, 42, 459-463.
- [12] T Jeevanand, N H Kim, J H Lee, B Siddaramaiah, M V Deepa Urs, and C Ranganathaiah, Investigation of Multi-Walled Carbon Nanotube Reinforced High-Density Polyethylene/Carbon Black Nanocomposites Using Electrical, DSC and Positron Lifetime Spectroscopy Technique, *Polymer International*, **2009**, 58, 775-780.

- [13] J H Lee, S K Kim, and N H Kim, Effects of the Addition of Multi-Walled Carbon Nanotubes on the Positive Temperature Coefficient Characteristics of Carbon Black- Filled High-Density Polyethylene Nanocomposites, *Scripta Materials*, **2006**, 55, 1119-1122.
- [14] Anju Gupta and Veena Choudhary, Electromagnetic Interference Shielding Behavior of Poly [Trimethylene Terephthalate]/Multi-Walled Carbon Nanotube Composites, *Composite Science and Technology*, **2011**, 71, 1563-1568.
- [15] N J S Sohi, M Rahaman, and D Khastgir, Dielectric Property and Electromagnetic Interference Shielding Effectiveness of Ethylene Vinyl Acetate-Based Conductive Composites: Effect of Different Type of Carbon Fillers, *Polymer Composite*, **2011**, 32, 1148-1154.
- [16] L L Vovchenko, L Y Matzui, V V Oliynyk, and V L Launetz, The Effect of Filler Morphology and Distribution on Electrical and Shielding Properties of Graphite-Epoxy Composites, *Molecular Crystals and Liquid Crystals*, **2011**, 535, 179-188.
- [17] J S Im, G J Kim, T Bae, and Y Lee, Effect of Heat Treatment on ZrO₂-Embedded Electro spun Carbon Fibers used for Efficient Electromagnetic Interference Shielding, *Journal of Physics and Chemistry of Solids*, **2011**, 72, 1175-1179.
- [18] M H Al-Saleh, and U Sundararaj, Electrically Conductive Carbon Nanofiber/Polyethylene Composite: Effect of Melt Mixing Conditions, *Polymer Advanced Technology*, **2011**, 22, 246-253.
- [19] S Wen, and D D L Chung, Pitch-Matrix Composites for Electrical, Electromagnetic and Strain-Sensing Applications, *Journal of Material Science*, **2005**, 40, 3897-3903.
- [20] A Das, H T Hatvaci, M K Tiwari, I S Bayer, D Erricolo, and C M Megaridis, Super Hydrophobic and Conductive Carbon Nanofiber/PTFE Composite Coatings for EMI Shielding. *Journal Colloid Interface Science*, **2011**, 353, 311–315.
- [21] N C Das, D Khastgir, T K Chaki, and A Chakraborty, Electromagnetic Interference Shielding Effectiveness of Carbon Black and Carbon Fibre Filled EVA and NR Based Composites, *Composites Part A: Applied Science and Manufacturing*, **2000**, 31, 1069-1081.
- [22] V Eswaraiah, V Sankaranarayanan, and S Ramaprabhu, Functionalized Graphene–PVDF Foam Composites for EMI Shielding, *Macromolecular Materials and Engineering*, **2011**, 296, 894-898.
- [23] S H Park, P Theilmann, K Yang, A M Rao, and P R Bandaru, The Influence Of Coiled Nanostructure on The Enhancement of Dielectric Constants and Electromagnetic Shielding Efficiency in Polymer Composites, *Applied Physics Letter*, **2011**, 96, 043115-043115.
- [24] Y Yang, M C Gupta, K L Dudley, and R W Lawrence, Novel Carbon Nanotube–Polystyrene Foam Composites for Electromagnetic Interference Shielding, *Nano Letters*, **2005**, 5, 2131-2134.
- [25] T Jeevananda, Siddaramaiah, and J H Lee, Synthesis and Characterization of Multiwalled Carbon Nanotube Doped Polyaniline Nanocomposites using Anionic Surfactant, *Polymer Advanced Technology*, **2008**, 19, 1754-1762.
- [26] B Philip, J N Xie, J K Abraham, and V K Varadan, Polyaniline / Carbon Nanotube Composites: Starting with Phenyl Amino Functionalized Carbon Nanotubes, *Polymer Bulletin*, **2005**, 53, 127-138.
- [27] M N Chandrashekar and C Ranganathaiah, Diffusion of Permanent Liquid Dye Molecules in Human Hair Investigated By Positron Lifetime, *Colloids and Surfaces B: Biointerfaces*, **2009**, 69, 129-134.
- [28] C Ranganathaiah and G N Kumaraswamy, New Method of Determining Miscibility in Binary Polymer Blends Through Hydrodynamic Interaction: The Free Volume Approach, *Journal of Applied Polymer Science*, **2009**, 111, 577-588.
- [29] C W Bunn, In fires from synthetic polymers, *Hill R (ed) Elsevier, Amsterdam*, **1953**, pp, 240-300.
- [30] M Bevis and E B Crellin, The Geometry of Twinning and Phase Transformations in Crystalline Polyethylene, *Polymer*, **1971**, 12, 666-684.
- [31] C J Li, A Ohmori and Y J Harada, Formation of an Amorphous Phase in Thermally Sprayed WC-Co, *Thermal Spray Technology*, **1996**, 5, 69-73.
- [32] N Parvin, M S Ullah, M F Mina and M A Gafur, Structures and Mechanical Properties of Talc and Carbon Black Reinforced High Density Polyethylene Composites: Effects of Organic and Inorganic Fillers, *Journal of Bangladesh Academy of Science*, **2013**, 37, 11-20.
- [33] L A Utracki and T Sedlacek, Free Volume Dependence of Polymer Viscosity, *Rheologica Acta*, **2007**, 46, 479–494.
- [34] B Wunderlich, Macromolecular Physics, Volume 3: Crystal Melting, *Academic Press: New York*, **1980**.
- [35] J Zhu, S Wei, Y Li, L Sun, N Haldolaarachchige, D P Young, C Southworth, A Khasanov, Z Luo, and Z Guo, Surfactant-Free Synthesized Magnetic Polypropylene Nanocomposites: Rheological, Electrical, Magnetic, and Thermal Properties, *Macromolecules*, **2011**, 44, 4382-4391.
- [36] J Yang, C Wang, K Wang, Q Zhang, F Chen, R Du and Q Fu, Direct Formation of Nano hybrid Shish-Kebab in the Injection Molded Bar of Polyethylene/Multiwalled Carbon Nanotubes Composite *Macromolecules*, **2009**, 42, 7016-7023.
- [37] S L Kodjie, L Li, B Li, W Cai, C Y Li and M J Keating, Morphology and Crystallization Behavior of HDPE/CNT Nanocomposite, *Journal of Macromolecular Science, Part B: Physics*, **2006**, 45, 231-245.

- [38] M K Seo, J R Lee and S J Park, Crystallization Kinetics and Interfacial Behaviors of Polypropylene Composites Reinforced with Multi-Walled Carbon Nanotubes, *Material Science and Engineering*, **2005**, 404, 79-84.
- [39] M K Seo and S J Park, A Kinetic Study on the Thermal Degradation of Multiwalled Carbon Nanotubes Reinforced Poly [Propylene] Composites, *Macromolecular Materials and Engineering*, **2004**, 289, 368-374.
- [40] Z Rimska, V Kresalek and J Spacek, AC Conductivity of Carbon Fiber-Polymer Matrix Composites at the Percolation Threshold, *Polymer Composites*, **2002**, 23, 95-103.
- [41] V Choudhary, S K Dhawan and P Saini, In EM Shielding-Theory and Development of New Materials, Jaroszewski M, Ziaja J [eds]. *Research Signpost*, **2012**, pp, 64-100.
- [42] S Bhadra, N K Singha and D Khastgir, Semi-Conductive Composites from Ethylene 1-Octene Copolymer and Polyaniline Coated Nylon 6: Studies on Mechanical, Thermal, Processability, Electrical and EMI Shielding Properties, *Polymer Engineering and Science*, **2008**, 48, 995-1006.
- [43] K Lakshmi, H John, K T Mathew, R Joseph and K E George, Microwave Absorption, Reflection and EMI Shielding of PU-PANI Composite, *Acta Materialia*, **2009**, 57, 371-375.
- [44] P K Pramanik, T N Saha and D Khastgir, Electromagnetic Interference Shielding by Conductive Nitrile Rubber Composites Containing Carbon Fillers, *Journal of Elastomers and Plastics*, **1991**, 23, 345-361.
- [45] Y Huang, N Li, Y Ma, F Du, F Li, X He, X Lin, H Gao and Y Chen, The Influence of Single-Walled Carbon Nanotube Structure on the Electromagnetic Interference Shielding Efficiency of its Epoxy Composites, *Carbon*, **2007**, 45, 1614-1621.
- [46] M S Ahmad, M K Abdelazez and A M Zihlif, Microwave Properties of the Talc Filled Polypropylene, *Journal of Material Science*, **1989**, 24, 1795-1800.
- [47] M Rahaman, T K Chaki and D Khastgir, Development of High Performance EMI Shielding Material from EVA, NBR, and Their Blends: Effect of Carbon Black Structure, *Journal of Material Science*, **2011**, 46, 3989-3999.
- [48] G T Mohanraj, T K Chaki, A Chakraborty and D Khastgir, AC Impedance Analysis and EMI Shielding Effectiveness of Conductive SBR Composites, *Polymer Engineering and Science*, **2006**, 46, 1342-1349.
- [49] J Liu, Y C Jean and H Yang, Free-Volume Hole Properties of Polymer Blends Probed by Positron Annihilation Spectroscopy: Miscibility, *Macromolecules*, **1995**, 28, 5774-5779.
- [50] P Kirkegaard, N J Pedersen and M Eldrup, Analysis of Bif₂ Poly Epoxy Resins, *Risoe National Lab. Denmark M-2740*, **1989**.
- [51] H Nakanishi, S J Wang and Y C Jean, In Proceedings of the International Symposium on Positron Annihilation Studies in Fluids, *World Scientific, Singapore*, **1988**.
- [52] S J Tao, Positronium Annihilation in Molecular Substances, *Journal of Chemical Physics*, **1972**, 56, 5499-5510.
- [53] M Eldrup D Lightbody and J N Sherwood, The Temperature Dependence of Positron Lifetimes in Solid Pivalic Acid, *Chemical Physics*, **1981**, 63, 51-58.
- [54] J M Raj and C Ranganathaiah, A New Method of Stabilization and Characterization of the Interface in Binary Polymer Blends by Irradiation: A Positron Annihilation Study, *Journal of Polymer Science Part B: Polymer Physics*, **2009**, 47, 619-632.
- [55] Anju Gupta and Veena Choudhary, Electrical Conductivity and Shielding Effectiveness of Poly [Trimethylene Terephthalate]/Multiwalled Carbon Nanotube Composites, *Journal of Material Science*, **2011**, 46, 6416-6423.